Diverse Population-Bursting Modes of Adapting Spiking Neurons

Guido Gigante,[1,*] Maurizio Mattia,[1] and Paolo Del Giudice[1,2]

[1]*Department of Technologies and Health, Istituto Superiore di Sanità, Viale Regina Elena 299, 00161 Roma, Italy*[†]

[2]*INFN, sezione Roma1, Piazzale Aldo Moro 2, 00185 Roma, Italy*

(Received 20 October 2006; published 4 April 2007)

We study the dynamics of a noisy network of spiking neurons with spike-frequency adaptation (SFA), using a mean-field approach, in terms of a two-dimensional Fokker-Planck equation for the membrane potential of the neurons and the calcium concentration gating SFA. The long time scales of SFA allow us to use an adiabatic approximation and to describe the network as an effective nonlinear two-dimensional system. The phase diagram is computed for varying levels of SFA and synaptic coupling. Two different population-bursting regimes emerge, depending on the level of SFA in networks with noisy emission rate, due to the finite number of neurons.

DOI: 10.1103/PhysRevLett.98.148101 PACS numbers: 87.19.La, 05.45.Xt, 87.18.Sn

Global oscillations and synchronization emerging in large populations of coupled oscillators are widely studied for their relevance in fields ranging from physics to biology. In particular, synaptically coupled network of neurons spontaneously show both regular and irregular bursts of activity which, besides playing a role in the developmental stages [1], are thought to complement rate-based coding in information transmission [2,3]. Among several effects involved in promoting and sustaining bursting [4], a prominent role is played by spike-frequency adaptation (SFA), by which a neuron receiving a sustained stimulation gradually lowers its firing rate. Slow potassium currents are thought to play a major role in SFA [4], and a first step in modeling SFA involves an additional calcium-gated potassium current I_{AHP}, temporarily hyperpolarizing the cell upon spike emission, with a recovery time of the order of hundreds of milliseconds [5]. Several theoretical approaches have investigated the collective behavior of population of integrate and fire (IF) neuron models including SFA [6]. Bursting activity can emerge from the competition between the recurrent synaptic excitation and the self-inhibition induced by adaptation, as proven using both simulations, phase-space analysis of phenomenological rate equations [7] and mean-field approaches both in fully connected networks [8] and in sparsely connected noisy networks [9]. The resulting bursting phenomenology is reminiscent of a *relaxation oscillator*: a stable high-rate fixed point is destabilized by SFA via a saddle-node bifurcation, bringing the network down to a low fixed point that takes over; with time, the level of SFA decreases, until the low fixed point gets in turn destabilized, again via a saddle-node bifurcation, and the cycle restarts. This behavior seems to be coherent with experimental findings from cultured networks of nervous cells [9,10].

In this Letter we show that several pieces of the available theoretical understanding summarized above can be integrated in a unifying approximate formulation; more importantly, the theory predicts, in addition to the bursting induced by bistability mentioned above, a regime in which population ''spikes'' appear if the firing rate crosses a threshold, in a way reminiscent of the single neuron excitability described by Fitzhugh and Nagumo *et al.* [11]. In the presence of finite-size fluctuations, the two bursting regimes exhibit different statistical properties, in terms of both the interburst interval distribution, and the duration of bursts, as a function of the level of adaptation and the intensity of synaptic coupling.

Reduced dynamics of coupled noisy adapting neurons.—We consider a network of N IF neurons with constant leakage, bounded membrane potential (the VLSI IF neurons [12], VIF in the following) and SFA modeled as an after-hyperpolarization current. The membrane potential V_i and the calcium concentration C_i of the ith neuron evolve as $\dot{V}_i = -\beta - gC_i + \sum_{kj} J_{ij}\delta(t - t_k^j - \delta_{ij}) + I_i^{\mathrm{ext}}$ and $\dot{C}_i = -C_i/\tau_c + \sum_k \delta(t - t_k^i)$, where β is the constant leakage, τ_c is the characteristic time of the calcium integration, $i, j = 1, \ldots N$ label the neurons, $\{J_{ij}\}$ are the efficacies of the (instantaneous) excitatory synapses, δ_{ij} are the delays for $\{j \to i\}$ spikes, and t_k^j is the time of the kth spike emitted by the jth neuron. The network is sparsely connected; for each neuron, ϵN nonzero J_{ij} are extracted from a truncated Gaussian distribution with mean J and variance $J^2\Delta^2$. I_i^{ext} is a Gaussian external current with moments μ_{ext} and σ_{ext}^2, and then single neurons are stochastic dynamical systems. V_i is constrained to the $(0, \theta)$ interval and when it crosses the threshold θ a spike is emitted.

Assuming a large number of synaptic contacts per neuron and a small average synaptic efficacy, the diffusion and mean-field approximations allow us to describe the stochastic system through a bidimensional nonlinear *Fokker-Planck* (FP) equation, with appropriate boundary conditions, for the evolution of the probability density function (PDF) $p(v, c, t)$, as described in [13] for the single neuron case. τ_c is supposed to be much longer than the average interspike interval, so $C_i(t)$ filters out the fluctuations of the single neuron activity, and can be well approximated by the

 © 2007 The American Physical Society

population average, $c(t)$. $p(v, c, t)$ then collapses, at each instant, in a one-dimensional subspace parallel to the v direction, and the system is well described by a one-dimensional FP equation, in which $c(t)$ appears as a parameter, that will depend on the instantaneous emission rate $\nu(t)$ (the probability current across the emission threshold). The ν-dependent moments of the Gaussian current driving the FP equation are $\mu = -\beta - gc + \epsilon NJ\nu + \mu_{\text{ext}}$ and $\sigma^2 = \epsilon NJ^2(1 + \Delta^2)\nu + \sigma^2_{\text{ext}}$.

Projecting the PDF on the moving basis of the eigenfunctions $|\phi_k\rangle$ of the one-dimensional FP operator [14,15] leads to the following matrix *emission rate equation* for the network population activity $\nu(t)$:

$$\begin{aligned} \dot{\vec{a}} &= (\mathbf{\Lambda} + \mathbf{M}\dot{\mu} + \mathbf{S}\dot{\sigma}^2)\vec{a} + \vec{m}\,\dot{\mu} + \vec{s}\dot{\sigma}^2, \\ \nu &= \Phi + \vec{f}\cdot\vec{a}, \qquad \dot{c} = -c/\tau_c + \nu, \end{aligned} \tag{1}$$

where all the functions depend explicitly only on $\nu(t)$ and $c(t)$. The infinite vector $\vec{a}$ gives the projection of $p(v, t)$ on the moving basis. $\{\vec{f}\}_k \equiv 1/2\sigma^2\partial_v|\phi_k\rangle|_{v=\theta}$ are the contributions of the nonstationary modes of the FP operator to $\nu(t)$ and Φ is the stationary current-to-rate gain function [12]. $\mathbf{\Lambda}$ is the infinite diagonal matrix of the (possibly complex) eigenvalues λ_k associated to $|\phi_k\rangle$, whereas the terms $\mathbf{M}\dot{\mu}$ and $\mathbf{S}\dot{\sigma}^2$ express the couplings between nonstationary modes ($\{\mathbf{M}\}_{kl} \equiv \langle\partial_\mu\psi_k|\phi_l\rangle$ and $\{\mathbf{S}\}_{kl} \equiv \langle\partial_{\sigma^2}\psi_k|\phi_l\rangle$, where $\langle\psi_k|$ are the eigenfunctions of the adjoint FP operator); in the interesting regimes, $\mathbf{\Lambda}$ turns out to be *a posteriori* dominant with respect to $\mathbf{M}\dot{\mu}$ and $\mathbf{S}\dot{\sigma}^2$ contributions, which will be thus neglected in the following, only for computational convenience. $\vec{m}\,\dot{\mu}$ and $\vec{s}\dot{\sigma}^2$ are the coupling terms between stationary and nonstationary modes ($\{\vec{m}\}_k \equiv \langle\partial_\mu\psi_k|\phi_0\rangle$ and $\{\vec{s}\}_k \equiv \langle\partial_{\sigma^2}\psi_k|\phi_0\rangle$) [15,16].

In Eq. (1) we can again distinguish the fast dynamics of the neurons membrane potentials related to $\vec{a}$, mainly related to dominant terms in $\mathbf{\Lambda}^{-1}$, typically of order of few milliseconds or less, and the slow one of c, with characteristic time τ_c (up to hundreds of milliseconds). Although the two cooperate in determining the dynamics of ν, the projections $\vec{a}$, which are in general nonzero, adapt almost instantaneously to changes in ν and c. This amounts to safely accepting the approximation $\dot{\vec{a}} \equiv 0$ in Eq. (1). More precisely it is assumed that $|\vec{f}\cdot\vec{w}| \gg |\vec{f}\cdot\mathbf{\Lambda}^{-1}\dot{\vec{w}}|$, where $\vec{w} \equiv \vec{m}\,\dot{\mu} + \vec{s}\dot{\sigma}^2$ is the forcing term for the dynamics of $\vec{a}$ in Eq. (1). Considering only the first, slowest nonstationary modes, the approximation reduces to $\tau_c \gg 1/|\text{Re}\lambda_1|$.

We remark that a naïve, fully adiabatic approximation would make $p(v, c, t)$ coincide for each t with the stationary PDF determined by the instantaneous value of ν and c ($\vec{a} = 0$); in the approximation we adopt, which is made possible by the spectral formulation in Eq. (1), the system is out of equilibrium, as long as ν and c vary ($\vec{a} \neq 0$ and can be large), and the moving basis follows instantaneously $\nu(t)$ and $c(t)$.

In this approximation Eq. (1) can be cast in the form

$$\tau_\nu\dot{\nu} = \Phi^{(\text{eff})} - \nu \qquad \dot{c} = -c/\tau_c + \nu \tag{2}$$

where $\tau_\nu = \gamma_1/(1 - \gamma_2)$ and $\Phi^{(\text{eff})} = (\Phi - c\gamma_2/\tau_c)/(1 - \gamma_2)$, with $\gamma_1 = \vec{f}\cdot\mathbf{\Lambda}^{-1}(\vec{m}\partial_\nu\mu + \vec{s}\partial_\nu\sigma^2)$ and $\gamma_2 = g\vec{f}\cdot\mathbf{\Lambda}^{-1}\vec{m}$. The series depend on the network connectivity and the average delay $\langle\delta_{ij}\rangle$. In particular, $\Phi^{(\text{eff})}$ is the effective stationary current-to-rate gain function in presence of adaptation. In the absence of synaptic coupling, when $\tau_\nu = 0$, Eq. (2) reduces to an expression similar to the one reported in [17], in which a fully adiabatic approximation is adopted. The method described and the reduction performed are valid for a wide class of IF neurons; the detailed behavior of the resulting equations however can change, and a model-dependent analysis is needed for quantitative predictions.

We have therefore reduced the stochastic dynamics of the system to a bidimensional nonlinear dynamical system, evolving in the (c, ν) plane. The left panel in Fig. 1 shows a sample orbit from Eq. (2) (black solid line) which well predicts the limit cycle observed in a simulation of $N = 10^4$ interacting VIF neurons (gray solid line). We stress again that the dynamics described by Eq. (2) differs from other "first order" approaches (as described by Wilson and Cowan [18]) in its state dependence of the time constant τ_ν, as can be seen in the right panel of Fig. 1 where τ_ν vs ν is plotted for three different c values. This is due to having projected $p(v, c, t)$ on a moving, rather than fixed, basis, and makes it possible for Eq. (2) to describe well a rich repertoire of dynamical states, as we will argue in the following. The nonmonotonic dependence on ν and the wide range spanned confirms that a quantitative description of the system's *global* dynamics would not be obtained from simpler approaches with constant characteristic times.

System phases and bifurcations.—To study the dynamical states accessible to the system we explore the plane spanned by g, the "level" of SFA, and the excitatory synaptic coupling J, which is proportional to the adimensional quantity $\Phi' \equiv \partial\Phi/\partial\nu$. The stability boundaries of available collective states are illustrated in Fig. 2, together

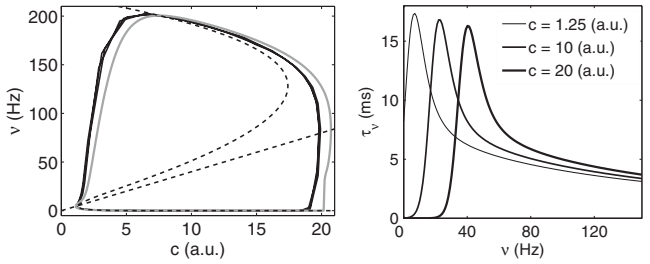

FIG. 1. Left panel: sample orbit from Eq. (2) (gray solid line) and from simulations (black solid line), and nullclines of Eq. (2) (dashed lines). Right panel: the τ_ν characteristic time appearing in Eq. (2) is plotted vs ν for three values of c (vertical sections of the phase plane on the left).

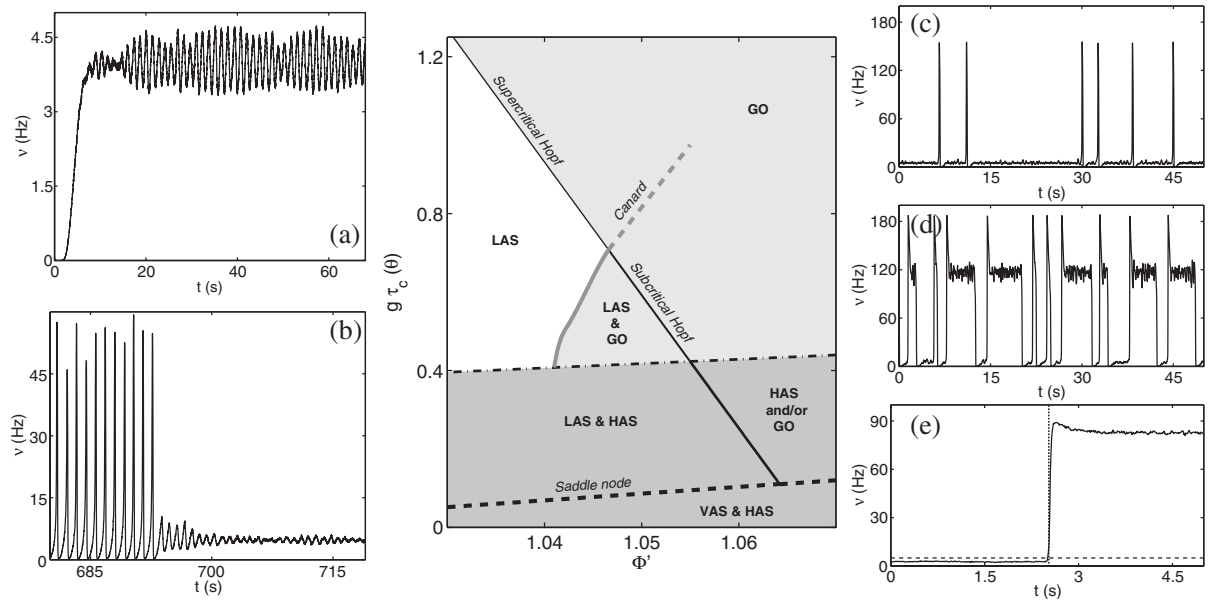

FIG. 2. Phase diagram of the reduced system of Eq. (2) in the $(\Phi', g\tau_c)$ plane (central panel). Shaded regions and bifurcation lines are described in the text. Lateral panels (a)–(e) illustrate typical time courses of $\nu(t)$ from simulations of N interacting VIF neurons: (a) GO; (b) LAS and GO; (c) LAS close to the LAS and GO region; (d) LAS and HAS; (e) VAS and HAS (dashed line: unstable fixed point at 5 Hz; dotted line: time of a brief external stimulation). $N = 10^3$ unless for (a) $N = 5 \times 10^5$ and (b) $N = 25 \times 10^3$.

with sample plots of the corresponding network activity from simulations [19].

All points in the plane are chosen adjusting network parameters to have a fixed point, stable or not, at $\nu = 5$ Hz with the same μ and σ^2. Hopf and saddle-node bifurcation lines are computed studying the Jacobian of Eq. (2). In the white region of the central panel in Fig. 2, hereafter named LAS (low-rate asynchronous state), the 5 Hz fixed point is the only state available and is stable. Crossing from left the gray solid line a stable global oscillatory state appears (GO) in addition to LAS: the two are simultaneously stable in the LAS and GO region, and finite-size fluctuations can make the network switch between the two. The bifurcation separating the LAS and LAS and GO regions is evaluated by testing, through a numerical integration of Eq. (2), the existence of a limit cycle around the asynchronous state. As an illustration, panel (b) shows a network in the LAS and GO region undergoing large global oscillations until a fluctuation makes it decay to the LAS. We remark that the observed bursts are genuine population oscillations: by integrating $\nu(t)$ across a burst, it can be verified that almost all neurons are recruited.

For high enough recurrent excitation Φ', increasing g results in stronger self-inhibition which promotes oscillations: LAS is destabilized and the system crosses a Hopf bifurcation, beyond which a global oscillatory state is the only stable attractor (GO light gray region). Entering the GO border from the LAS or the LAS and GO the system crosses a *supercritical* or *subcritical* Hopf bifurcation line, respectively, as proven by the evaluation of a third order expansion of Eq. (2) around the fixed point at 5 Hz. Panel (a) illustrates the oscillatory activity of a network just beyond the supercritical Hopf bifurcation. In the region close to the Hopf bifurcation line, crossing from above the dashed line the system exhibit a "Canard bifurcation," by which the radius of the system orbits in the phase plane abruptly increases.

For low g, and not too high Φ', the system does not exhibit global oscillations. In the LAS and HAS (for high-rate asynchronous state) gray region two asynchronous stable fixed points coexist. Again, finite-size fluctuations can make the system alternate between the two, as illustrated in panel (d) (notice the ν overshoot when leaving the LAS state for HAS, due to the temporarily low level of $c(t)$, and the transient very low rate when returning abruptly to LAS, due to the high self-inhibition level). For very low g, where adaptation has a negligible effect, increasing Φ', with constant g, the system crosses a saddle-node bifurcation line, beyond which LAS is destabilized and VAS (very low-rate asynchronous state) takes over. Panel (e) illustrates the dynamics in the VAS and HAS region: starting from a VAS, driven by a stimulation at $t = 2.5$ s, the network moves to a HAS.

Two bursting regimes.—The shape of the nullclines of Eq. (2) and the above discussion would suggest that our effective 2D nonlinear system should share with Fitzhugh-Nagumo neuron models key features like the excitability which allows the onset of the action potentials. Intuition suggests, and simulations confirm, that the region of excitability is a portion of the LAS phase, close enough to the LAS and GO border, where the global oscillatory state is

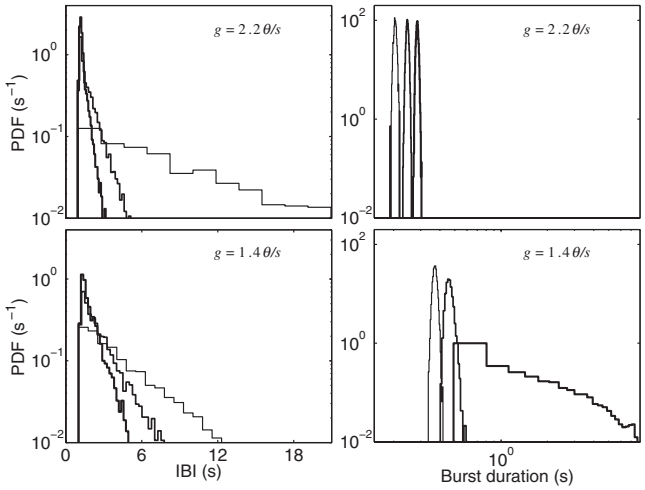

FIG. 3. IBI (left panels) and burst duration (right panels) distributions from simulations of 10^3 interacting VIF neurons for low (bottom panels) and high (top panels) level of SFA, at different synaptic coupling strength: from thin to tick lines $\Phi' = \{0.95, 1.015, 1.06\}$ (top); $\Phi' = \{0.96, 0.99, 1.015\}$ (bottom). In all cases $\tau_c = 0.25$ s.

not stable yet, but the system can be very easily driven to wild ν excursions by finite-size fluctuation crossing a suited threshold. In Fig. 2, panel (c), it is seen that, irregularly in time (it is a fluctuation driven process) the network produces "spikes." For lower levels of SFA the type of bursting behavior discussed in [7–9] appears [see an example in panel (d) of Fig. 2].

The two bursting regimes exhibit different statistical properties of the interburst intervals (IBI) and the duration of the bursts, as Fig. 3 illustrates. Left panels show IBI distributions sampled for low (bottom) and high (top) g. Increasing thickness of the solid lines indicates increasing Φ'. For the higher g, which corresponds to a regime of excitability, higher Φ' imply getting closer to the LAS and GO border, and the system goes from a regime of very irregular, rare bursting (essentially Poissonian IBI distribution), to more frequent and regular bursting (the IBI distribution shrinks shifting to the left). For the bursting regime related to bistability (lower g value), the IBI distribution is less sensitive to Φ': for higher Φ' the basin of attraction of the lower state shrinks, so bursting gets more frequent, but it remains essentially a Poisson-like process. The two panels on the right describe how the distribution of the bursts duration varies with Φ' for the two levels of SFA. The top panel shows that in the excitable regime bursts are brief and their duration does not depend much on Φ', while for the lower g, as the higher state gets more and more stable the time the network spends there is longer, which makes the burst duration distribution spread significantly.

Such diverse bursting modes could be tested in principle in cultured nervous cells grown on multielectrode arrays [20,21]: the control of, e.g., the cell density and the connectivity level, and the pharmacological manipulations modulating both synaptic efficacy and SFA, could allow the exploration of an equivalent phase plane, aiming at a quantitative link with the theory.

We acknowledge the support of the EU grant No. IST-2001-38099.

*Also at Dept. of Physics, University "La Sapienza," Piazzale A. Moro 5, 00161 Roma, Italy.
†Web site: http://neural.iss.infn.it

[1] Y. Ben-Ari, Trends Neurosci. **24**, 353 (2001); L. I. Zhang and M. M. Poo, Nat. Neurosci. **4**, S1207 (2001); M. Corner, J. van Pelt, P. S. Wolters, R. E. Baker, and R. H. Nuytinck, Neurosci. Biobehav. Rev. **26**, 127 (2002).
[2] J. E. Lisman, Trends Neurosci. **20**, 38 (1997).
[3] F. Gabbiani, W. Metzner, R. Wessel, and C. Koch, Nature (London) **384**, 564 (1996); A. M. Oswald, M. J. Chacron, B. Doiron, J. Bastian, and L. Maler, J. Neurosci. **24**, 4351 (2004);N. A. Lesica and G. B. Stanley, J. Neurosci. **24**, 10 731 (2004).
[4] M. Stocker, Nat. Rev. Neurosci. **5**, 758 (2004).
[5] C. Koch, *Biophysics of Computation* (Oxford University Press, New York, 1999).
[6] D. Golomb and Y. Amitai, J. Neurophysiol. **78**, 1199 (1997); X.-J. Wang, J. Neurophysiol. **79**, 1549 (1998); G. Fuhrmann, H. Markram, and M. Tsodyks, J. Neurophysiol. **88**, 761 (2002).
[7] P. E. Latham, B. J. Richmond, P. G. Nelson, and S. Nirenberg, J. Neurophysiol. **83**, 808 (2000).
[8] C. van Vreeswijk and D. Hansel, Neural Comput. **13**, 959 (2001).
[9] M. Giugliano, P. Darbon, M. Arsiero, H. R. Lüscher, and J. Streit, J. Neurophysiol. **92**, 977 (2004).
[10] P. E. Latham, B. J. Richmond, S. Nirenberg, and P. G. Nelson, J. Neurophysiol. **83**, 828 (2000).
[11] R. Fitzhugh, Biophys. J. **1**, 445 (1961); J. Nagumo, S. Animoto, and S. Yoshizawa, Proc. Inst. Radio Eng. **50**, 2061 (1962).
[12] S. Fusi and M. Mattia, Neural Comput. **11**, 633 (1999).
[13] G. Gigante, P. Del Giudice, and M. Mattia, Math. Biosci. doi:10.1016/j.mbs.2006.11.010 (2006).
[14] B. W. Knight, D. Manin, and L. Sirovich, in *Proceedings of SRC, Lille-France*, edited by E. C. Gerf (Cite Scientifique, Lille, France, 1996).
[15] M. Mattia and P. Del Giudice, Phys. Rev. E **66**, 051917 (2002).
[16] M. Mattia and P. Del Giudice, Phys. Rev. E **70**, 052903 (2004).
[17] J. Benda and A. V. Herz, Neural Comput. **15**, 2523 (2003).
[18] H. R. Wilson and J. D. Cowan, Biophys. J. **12**, 1 (1972).
[19] See EPAPS Document No. E-PRLTAO-98-077715 for a more detailed description of the theoretical approach, and a sample of trajectories from Eq. (2) in the different regions of Fig. 2. For more information on EPAPS, see http://www.aip.org/pubservs/epaps.html.
[20] S. Marom and G. Shahaf, Q. Rev. Biophys. **35**, 63 (2002).
[21] M. Canepari, M. Bove, E. Maeda, M. Cappello, and A. Kawana, Biol. Cybern. **77**, 153 (1997); R. Segev, Y. Shapira, M. Benveniste, and E. Ben-Jacob, Phys. Rev. E **64**, 011920 (2001).